Indonesian Journal of Pharmacy

VOL 37 (2) 2026: 390–402 | RESEARCH ARTICLE

Study of Formyl and Phenyl Substituted Styrylpyrazolines: Synthesis, *In Vitro* Antibacterial Evaluation, and Molecular Docking against DNA Gyrase

Artania Adnin Tri Suma[1,*], Norman Yoshi Haryono[2,3], Navista Sri Octa Ujiantari[1], Adhetya Kurnia Wicaksana[1], Anastacia Verena Salim[2], Cintya Nurul Apsari[1], Siti Nurul Hidayah[1], Syazwani Itri Amran[4] and Badra Sanditya Rattyananda[5,6]

1. Department of Pharmaceutical Chemistry, Faculty of Pharmacy, Universitas Gadjah Mada, Sekip Utara, Bulaksumur, Yogyakarta, 55281, Indonesia.
2. Biotechnology Study Program, Department of Applied Science, Faculty of Mathematics and Natural Sciences, Universitas Negeri Malang, Jl. Semarang No.5, Malang, 65145, Indonesia.
3. Health and Food Centre, Institute of Research and Community Services, Universitas Negeri Malang, Jl. Semarang No.5, Malang 65145, Indonesia.
4. Department of Biosciences, Faculty of Science, Universiti Teknologi Malaysia, Johor Bahru 81310, Johor, Malaysia
5. Research Centre for Computation, Research Organization for Electronics and Informatics, National Research and Innovation Agency (BRIN), Jl. Tamansari 71, Bandung City, 40132, Indonesia
6. Doctoral Program of Computational Science, Division of Mathematical & Physical Sciences, Graduate School of Science & Technology, Kanazawa University, Kakuma, Kanazawa, Ishikawa, 920-1192, Japan

Article Info

Submitted: 15-03-2025
Revised: 29-07-2025
Accepted: 04-08-2025

*Corresponding author:
Artania Adnin Tri Suma

Email:
artania.adnin.t.s@ugm.ac.id

ABSTRACT

Bacterial resistance remains a persistent challenge to most antibiotics, urging the need to develop novel antibacterial agents. Styrylpyrazoline derivatives, previously reported to possess diverse bioactivities, were synthesized, and the antibacterial potential was studied. Styrypyrazolines 2a-2b were tested on five bacterial strains, namely Gram-positive *Staphylococcus aureus, Staphylococcus epidermidis, Bacillus subtilis,* as well as Gram-negative *Escherichia coli* and *Pseudomonas aeruginosa*. The *in vitro* evaluation was performed using disk diffusion and microdilution methods. The results revealed that compounds 2a and 2b had the highest inhibitory activity toward *S. aureus*. Compound 2b showed significantly lower MIC_{50} values due to the phenyl substituent existence at the N-1 position of the pyrazoline ring. In contrast, both compounds were inactive against *B. subtilis* and *S. epidermidis.* Molecular docking targeting DNA gyrase subunit B was performed to further investigate their antibacterial mechanism. It was revealed that the two compounds were found to interact with the receptor within the ATP-binding pocket. Similar to ciprofloxacin, compound 2a formed hydrogen bonds with the Asp81 residue, showing the potential as a DNA gyrase inhibitor. Compound 2b formed an aromatic-hydrogen bridge interaction with the Pro87 residue. This study suggests that styrypyrazolines 2a and 2b possess promising antibacterial activity. However, the potency is lower compared with the reference antibiotics. Further optimization is therefore necessary to enhance their potency as antibacterial agents.

Keywords: pyrazolines, gyrB inhibitor, antibacterial, *in silico*

INTRODUCTION

The rise of antibiotic resistance in overcoming bacterial infections has become a significant global health concern. This resistance often arises due to the incorrect use and overconsumption of antibiotic agents (Uddin et al., 2021), leading to the development of antimicrobial resistance (AMR), particularly bacterial AMR. In response to this challenge, medicinal chemistry studies have focused on exploring novel compounds with potent antibacterial activity (Ho et al., 2025).

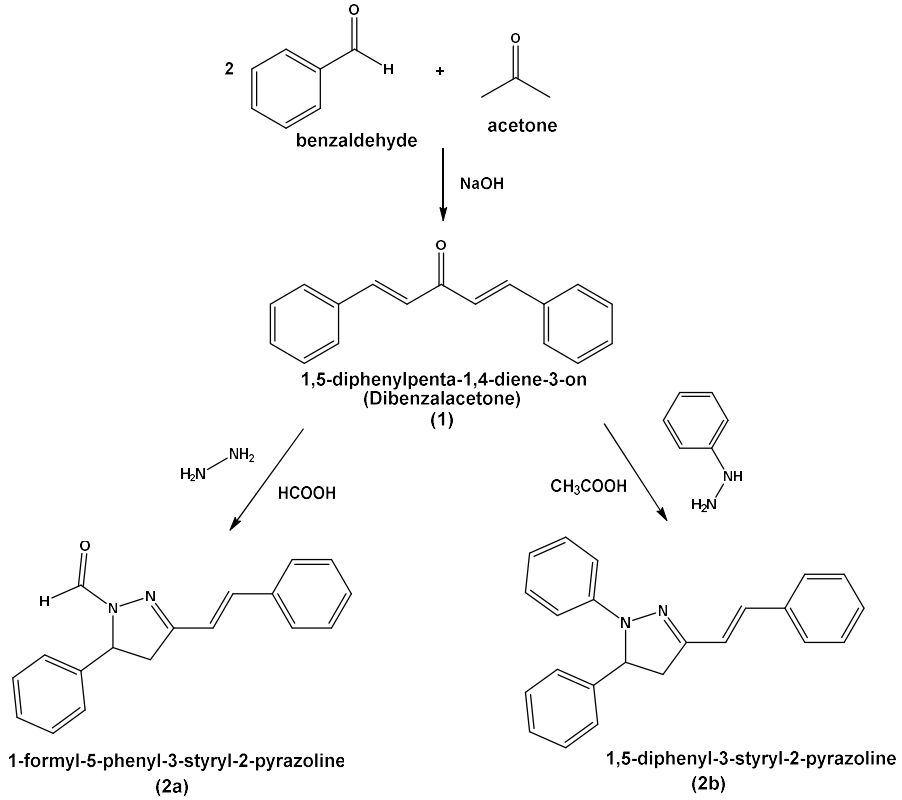

Figure 1. Synthetic route of styrylpyrazolines 2a-2b.

This strategy is in accordance with one of the global action plans established through the World Health Organization (WHO), that is increasing study and development on new medicines, especially those targeting priority pathogens (World Health Organization, 2019).

The discovery of therapeutic compounds through synthetic pathways offers the advantage of obtaining pure active substances. A group of compounds that have received substantial attention is nitrogen-containing heterocycles, owing to their structural diversity and wide-ranging pharmacological properties (Marshall et al., 2024). Therefore, these compounds have become important targets for synthetic organic chemistry research over the years. Various classes of synthetic antibacterial agents have been explored, including quinolones, carbapenems, and azoles (Shi et al., 2023). In recent years, pyrazoles and pyrazolines have gained interest due to their versatile biological profiles (Varghese et al, 2017; Yadav et al., 2024). Among them, styrylpyrazolines represent a promising but underexplored subclass. Despite their notable biological activities and intriguing physicochemical characteristics, including tautomerism, isomerism, and conjugation extension, along with their rich chemistry related to the synthesis and transformation, these compounds have rarely been studied (Gomes et al., 2020). This makes them an attractive target for further investigation.

Styrylpyrazoline derivatives have been shown in a few studies to possess antibacterial activity against a variety of bacterial species, including *Escherichia coli, Staphylococcus aureus,* and *Pseudomonas aeruginosa* (Gomes et al., 2020; Gressler et al., 2010). Structural modifications of pyrazolines at the N-1 position result in a wide variety of bioactivity alterations (Alex & Kumar, 2014). Substitutions at N-1 with formyl and phenyl groups have been shown to improve antibacterial activity (Sid et al., 2016; Sharma et al., 2013).

The target compounds in this study are styrylpyrazolines substituted at the N-1 position with formyl (compound 2a) and phenyl (compound 2b) groups (Figure 1). The *in vitro* antibacterial

activity was tested against selected bacterial strains. Compound 2a is rarely synthesized, and to date, the antibacterial activity has not been investigated against either Gram-positive or Gram-negative bacteria. On the other hand, compound 2b has been previously synthesized in several studies, but reports of the antibacterial evaluation remain limited, as it has only been tested against *Escherichia coli* and *Bacillus cereus* using a diffusion method that offered qualitative insight (Sharma et. al., 2013). Moreover, no data are available regarding the activity against other key pathogens such as *Staphylococcus aureus, Staphylococcus epidermidis, Bacillus subtilis,* and *Pseudomonas aeruginosa*. In this work, the antibacterial profiling of compounds 2a and 2b was expanded and conducted using a standardized microdilution method, allowing for a more quantitative assessment of antibacterial potency.

Computational chemistry is a crucial part of drug discovery, along with its development, supplementing experimental results. Molecular docking is a common method for predicting the correct orientation and conformation of a drug molecule when bound to its target receptor, offering insight into the stability and the formed drug-receptor complex interaction (Torres et al., 2019). In this analysis, molecular docking was performed to evaluate styrylpyrazoline derivatives interaction with bacterial DNA gyrase. This enzyme, a type II topoisomerase, serves an important function in bacterial DNA replication, transcription, as well as recombination processes, making it a promising target for antibacterial drug development (Adeniji et al., 2020). Furthermore, no earlier research has examined the antibacterial properties of the target styrylpyrazoline derivatives against DNA gyrase through molecular docking. This work addresses this gap by offering both experimental and computational insights into the antibacterial properties of the target compounds. Such molecular-level information may be valuable for subsequent optimization and development, particularly as computational approaches are increasingly being integrated into formulation and drug delivery research (Casalini, 2021; Cvijic et al., 2018).

MATERIALS AND METHODS

Synthesis

Chemicals and solvents were obtained from Sigma-Aldrich, including benzaldehyde, acetone, hydrazine hydrate, phenylhydrazine, glacial acetic acid, formic acid, ethanol, sodium hydroxide, hydrochloric acid, dichloromethane, ethyl acetate, n-hexane, methanol, and dimethyl sulfoxide (DMSO). The progress of synthesis reactions was assessed using thin-layer chromatography (TLC), carried out on silica gel 60 F254 precoated aluminum plates from Merck. UV light (λ 254 and 366 nm) to observe the TLC result was obtained from the CAMAG UV Cabinet 4. Furthermore, densitometry analysis was performed in CAMAG TLC Scanner 4. Column chromatography was employed using silica gel from Merck. Solvent evaporation was then conducted using Dibby Specific Stuart RE300 Rotary Evaporator with Stuart RE300DB digital water bath and B-ONE SHB-III water circulating vacuum pump. Melting points were determined using the Falc Cooling Melting Point Instrument MPD-03. Mass Spectrometry (ESI) was performed on a Sciex Triple Quadrapole 4500. Finally, FTIR Spectrometry was performed on Shimadzu Prestige-21 using KBr discs, and GC-MS was conducted using Shimadzu QP2010S (EI).

Synthesis of dibenzalacetone (1)

Dibenzalacetone (1) was prepared based on the literature with some modifications (Suma et al., 2019). Benzaldehyde (10 mmol, 1.02 mL) was dissolved in 10 mL of absolute ethanol and stirred for 5 min. Acetone (5 mmol, 0.23 mL) was introduced and the mixture was stirred for 15 min at 1-4 °C. Subsequently, a mixture of 10 mL of 20% (w/v) sodium hydroxide solution in water along with 5 mL of absolute ethanol was introduced dropwise at room temperature. The mixture was stirred for 60 min and monitored by TLC using dichloromethane:n-hexane (3:2). Furthermore, hydrochloric acid 10% (v/v) was introduced to the reaction until pH 6. The crude product was collected through filtration of the reaction mixture. It was then washed with cold water and dried. Recrystallization with ethanol:water 2:1 was done to obtain compound 1. FTIR spectrum (KBr), ν_{max} (cm^{-1}): 3052 (C_{sp2}-H str.), 1651 (C=O str.), 1626 (alkene C=C str.), 1590 and 1495 (aromatic C=C str.), 983 (*trans* alkene C_{sp2}-H *oop* bend), 762 and 695 (aromatic monosubs. C_{sp2}-H *oop* bend). Mass spectrum (EI), m/z: 234.2 (M^+).

Synthesis of 1-formyl-5-phenyl-3-styryl-2-pyrazoline (2a) and 1,5-diphenyl-3-styryl-2-pyrazoline (2b)

Styrylpirazolines 2a and 2b were synthesized according to the literature with some modifications (Suma & Wahyuningsih, 2023).

Dibenzalacetone (1) (2 mmol, 0.469 g) was dissolved in 5 mL formic acid, and then 2 mL hydrazine hydrate was added. The reaction was performed in a reflux system for 4 h, assessed by TLC with chloroform. The reaction mixture was maintained at 4 °C overnight. The product was then purified by filtration, rinsed with methanol, and dried to yield compound 2a. FTIR spectrum (KBr), ν_{max} (cm^{-1}): 3109 (C_{sp2}-H str.), 2916 (C-H str.), 2800 and 2708 (aldehyde C_{sp2}-H str.), 1651 (C=N str.), 1635 (alkene C=C str.), 1620 (C=O str.), 1604 and 1481 (aromatic C=C str.), 1226 (C-N str.), 1450 (-CH_2- bend). Mass spectrum (EI), m/z: 234.2 (M^+, 20%), 233.1 (40), 131.1 (100), 103.1 (60), 91.1 (20). Mass spectrum (ESI), m/z: 277 $(M+H)^+$.

Dibenzalacetone (1) (2 mmol, 0.469 g) was dissolved in 5 mL glacial acetic acid, then 0.2 mL phenylhydrazine was introduced. For 4 h, the reaction was carried out in a reflux system under TLC monitoring with a 1:1 dichloromethane:n-hexane ratio. Then, it was transferred onto crushed ice and stored at 4 °C overnight. The product was filtered, rinsed with cold water, and dried. Subsequently, column chromatography was performed with an eluent gradient of *n*-hexane and dichloromethane, followed by evaporation to obtain compound 2b. FTIR spectrum (KBr), ν_{max} (cm^{-1}): 3024 (C_{sp2}-H str.), 2924 (C-H str.), 1651 (C=N str.), 1620 (alkene C=C str.), 1597 and 1496 (aromatic C=C str.), 1450 (-CH_2- bend), 1327 (C-N str.), 948 (*trans* alkene C_{sp2}-H *oop* bend), 748 and 694 (aromatic monosubs. C_{sp2}-H *oop* bend). Mass spectrum (EI), m/z: 234.2 (M^+, 20%), 233.1 (40), 131.1 (100), 103.1 (60), 91.1 (20). Mass spectrum (ESI), m/z: 325 $(M+H)^+$.

In vitro evaluation

Bacterial strains of *S. aureus, S. epidermidis, B. Subtilis, E. coli*, and *P. aeruginosa* were acquired from the collection of the Laboratory of Microbiology, Biology Department, Universitas Negeri Malang. The bacterial inoculum used for the *in vitro* test was from a stock culture grown in a tube containing Nutrient Agar (NA) medium. Each bacterial inoculum was then subcultured onto a petri dish containing 20 mL of NA medium and incubated at 37°C for 16-18 h. After incubation, a single colony from each bacterial culture was collected with an inoculation loop and moved into 10 mL of Nutrient Broth (NB) medium in a tube. The bacterial cultures were then incubated at 37 °C for 16-18 h. Afterwards, 2 mL of each bacterial culture was sampled and its optical density (OD) at 600 nm was determined. The bacterial cultures were then diluted using NB medium until they reached a concentration equivalent to 0.5 McFarland standard (OD600 = 0.08-0.1), indicating that the bacterial population was in the log phase of growth.

Disk diffusion, along with microdilution techniques, was used for the *in vitro* antibacterial assessment. The 20 mL of NA medium was formulated and added to Petri dishes for the disk diffusion procedure. To guarantee even distribution, the bacterial suspension was uniformly spread onto the solidified agar surface utilizing a sterile cotton swab. Paper disks containing 10 µL of the test sample (1000 µg/mL in DMSO 1%) were placed onto the inoculated agar surface. Then, it was incubated in an upside-down position at 37 °C for 18-24 h. To evaluate the antibacterial activity, the inhibition zones were identified. This method was performed for compounds 2a-b and ciprofloxacin as a positive control against all five bacterial strains. A solution of DMSO 1% was used as a negative control.

Compounds 2a-b were also evaluated using the microdilution technique according to the Clinical and Laboratory Standards Institute (CLSI) standard (CLSI, 2023) against four bacterial strains, namely *S. aureus, S. epidermidis, E. coli*, as well as *P. aeruginosa*. Both compounds were prepared in the concentration range of 3.2-819.2 µg/mL in DMSO 1%. Ciprofloxacin, used as the reference antibiotic, was tested at concentrations varying from 0.025 to 0.4 µg/mL in DMSO 1%. Into each well of 96-microplates was inserted 270 µL of bacterial suspension that had been diluted with Muller Hinton Broth (MHB) and 30 µL of the tested compound. Incubation was conducted at 37 °C for 24 hours. Growth control and solvent control were run in parallel with every test. A microplate reader was used to analyze the microplate and measure the absorbance at 600 nm wavelength. The inhibition percentage was determined utilizing the formula (Haney et al., 2021).

$$\%inhibition = \left(1 - \frac{Abs\ sample - Abs\ SC}{Abs\ GC - Abs\ SC}\right) x\ 100\%$$

where SC = sterile control and GC = growth control. The minimum concentration at which bacterial growth was inhibited by 50% (MIC50) was determined using SPSS version 26.

The microdilution method was performed in triplicate (n = 3), and MIC50 values were reported as the mean ± standard deviation (SD).

Table I. Physicochemical properties of synthesized compounds

Compound	Molecular Weight	Appearance	Solubility	Melting Point (°C)	Rf Value
1	234	Yellow solid	Soluble in DCM, ethanol, and methanol. Insoluble in water.	104-105	0.50 (DCM:hex 3:2) 0.95 (EtOAc:hex 2:1) 0.30 (DCM:hex 1:1)
2a	276	White solid	Slightly soluble in DMSO and water.	152-154	0.05 (EtOAc:hex 2:1)
2b	324	Light green solid	Soluble in DCM and acetone. Insoluble in water.	150-152	0.70 (DCM:hex 1:1)

The MIC50 data obtained were analyzed using one-way ANOVA (analysis of variance), with Tukey's post hoc test applied ($p < 0.01$ or $p < 0.05$).

Molecular docking

Docking protocols were developed with MOE v2022 (MOE, 2022) to predict the inhibitory activity of compounds 2a and 2b toward DNA gyrase. The 3D structure used in this docking was the ATP-binding site crystal structure in *S. aureus* DNA gyrase subunit B (GyrB) with PDB ID 5D6Q (Zhang et al., 2015). The native ligand was 1-ethyl-3-{4-[(E)-2-(pyridin-3-yl)ethenyl]-5-(1H-pyrrol-2-yl)-1,3-thiazol-2-yl}urea (57V). The protein structure was protonated, and the charge was assigned using the AMBER force field. Compounds 2a and 2b were built, and the potential energy function was calculated using MOPAC with PM3 as the parameter. Ciprofloxacin was prepared as well as a control positive in the docking. Redocking was performed to validate the docking protocol, and RMSD values were evaluated. The validated docking protocol was used to dock and evaluate the interaction of compounds 2a and 2b to the ATP domain of GyrB.

RESULTS AND DISCUSSION

Synthesis

Pyrazoline compounds can be synthesized through various types of reactions using different reactants. One of the most common strategies involves the reaction between α,β-unsaturated carbonyl compounds and hydrazine through a cyclocondensation reaction (Gomes et al., 2020). Hydrazine is frequently utilized as a reactant because it directly contributes its two nitrogen atoms to form the 2-pyrazoline ring structure (Vahedpour et al., 2021). Among the potential sources of α,β-unsaturated carbonyl compounds suitable for the synthesis of styrylpyrazolines is dibenzalacetone.

Dibenzalacetone can be prepared via an aldol condensation reaction between benzaldehyde and acetone with a basic catalyst to produce β-hydroxy carbonyl, which then can easily undergo dehydration to produce dibenzalacetone (compound 1) (Figure 1). The synthesized dibenzalacetone was obtained with a yield of 84.44%. The solubility test showed that this compound is easily dissolved in dichloromethane (DCM), ethanol, and methanol, but it is insoluble in water (Table I). TLC analysis with dichloromethane:*n*-hexane 3:2 as eluent showed that compound 1 can be observed under UV light (254 and 366 nm) with the Rf value of 0.5 and it appeared in a single spot (Supplementary Figure S1). This suggests that compound 1 was obtained in a qualitatively pure product. GC-MS (EI) analysis was performed to complement this finding. The chromatogram of GC-MS showed a peak with an area of 94.84% at the retention time of 38.95 min (Supplementary Figure S2). The mass spectrum of this peak showed a molecular ion (M^+) at m/z 234.2, corresponding to the molecular weight of compound 1 (234 g/mol) (Supplementary Figure S3). Compound 1 has a melting point of 104-105 °C and a boiling point of 280-286 °C. This melting point value suggests that this compound is in *the trans, trans* isomer (Houshia et al., 2019). FTIR analysis was conducted to further elucidate its structure. The FTIR spectrum showed that there is no C-H aldehyde absorption, proving that benzaldehyde, as the reactant, was no longer present. The C-H sp^3 absorption was also not observed, proving that acetone, as the reactant, was no longer present as well. The formation of compound 1 was shown by the absorption of C=C stretching at 1626 cm^{-1}. The presence of C-H sp^2 *trans* alkene absorption at 983 cm^{-1} further proved that compound 1 was obtained in the *trans* isomer (Supplementary Figure S4).

Styrylpyrazoline 2a was synthesized via cyclocondensation reaction from dibenzalacetone as the source of α,β-unsaturated carbonyl compounds and hydrazine hydrate with formic acid. Compound 2a was obtained with a yield of 89.13%. The solubility test showed that this compound is only slightly soluble in dimethyl sulfoxide (DMSO) and water. TLC analysis of compound 2a and 1 with ethyl acetate:*n*-hexane 2:1 as eluent showed that compound 2a can be observed under UV light (254 and 366 nm) with the Rf value of 0.05, and it appeared in a single spot. While compound 1 in this eluent appeared in Rf value of 0.95 (Supplementary Figure S5). This suggests that compound 2a was obtained in a qualitatively pure product. Compound 2a has a melting point of 152-154 °C (*cf*. Nassan et al., 2022, 120-122 °C) and a boiling point of over 240 °C. The higher melting point observed in this study may indicate different purity or different crystallization behaviour of the synthesized product. To further confirm the structure, mass spectrometric analysis was performed. However, due to the high boiling point value and thus low volatility of compound 2a, GC-MS (EI) analysis was not feasible. Instead, ESI-MS using a direct inlet was employed. The mass spectrum showed the $(M+H)^+$ peak at m/z 277, corresponding to the molecular weight of compound 2a (276 g/mol). This is consistent with the ESI-MS data reported by Singh et al. (2009). The FTIR spectrum showed no N-H stretching absorption, proving that hydrazine hydrate, as the reactant, is no longer present. The appearance of C-H sp^3 stretch at 2916.37 cm^{-1}, C-H aldehyde at 2800 and 2708 cm^{-1}, C=N stretch at 1651 cm^{-1}, C-N stretch at 1226 cm^{-1}, and CH_2 bend at 1450 cm^{-1} proved the formation of styrylpyrazoline 2a (Supplementary Figure S6). The FTIR data are also similar to those reported by Singh et al. (2009).

Styrylpyrazoline 2b was also synthesized using the same method. The difference is the use of phenylhydrazine as the reactant. Compound 2b was obtained with a yield of 66.27%. The solubility test showed that this compound was easily dissolved in dichloromethane and acetone but was insoluble in water. TLC analysis of compound 2b and 1 with dichloromethane:*n*-hexane 1:1 as eluent showed that compound 2b can be observed under UV light (254 and 366 nm) with the Rf value of 0.7 and it appeared in a single spot. While compound 1 in this eluent appeared at 0.3 (Supplementary Figure S7). This suggests that 2b was obtained in a qualitatively pure product. Compound 2b has a melting point of 150-152 °C, which is similar to the previously reported value (*cf*. Riham et al., 2020, 150-151 °C). This compound decomposed at over 210 °C. Thus, it was unable to be analyzed using GC-MS. Analysis using ESI-MS showed the presence of $(M+H)^+$ peak at m/z 325, which corresponded to the molecular weight of compound 2b (324 g/mol). The FTIR spectrum showed no C=O carbonyl stretch and no N-H stretch absorption, proving that both dibenzalacetone and phenylhydrazine, as the reactants, were no longer present. The appearance of C-H sp^3 stretch at 2924 cm^{-1}, C=N stretch at 1651 cm^{-1}, C-N stretch at 1327 cm^{-1}, and CH_2 bend at 1450 cm^{-1} proved the formation of styrylpyrazoline 2b (Supplementary Figure S8). The FTIR data are in agreement with the reported value by Sharma et al. (2013).

In vitro antibacterial evaluation

The synthesized styrylpyrazolines, 2a and 2b, were examined for their *in vitro* antibacterial activity by disk diffusion and microdilution methods. The first method was commonly used for initial screening purposes (Balouiri et al., 2016). The inhibition activity for both compounds was screened against five bacterial strains: *S. aureus, S. epidermidis, B. subtilis, E. coli*, and *P. aeruginosa.* The antibiotic ciprofloxacin was used as the standard antibiotic drug for positive control. Ciprofloxacin, a member of the quinolone class, was selected for its broad antibacterial spectrum and its mechanism of action that targets bacterial DNA gyrase (Hooper & Jacoby, 2016). It showed that ciprofloxacin exhibited the largest inhibition zones against all tested bacteria, confirming its broad-spectrum activity (Table IIA). The lack of inhibition by DMSO 1% confirmed that the solvent did not interfere with the antibacterial activity. Both compounds 2a and 2b showed inhibition zones ranging from 6 to 9 mm against four bacteria: *S. aureus*, *S. epidermidis, E. coli*, and *P. aeruginosa*. Based on the inhibition zones, the inhibition activity can be categorized as weak (<5 mm), moderate (5-10 mm), and strong (>10 mm) (Suma et al., 2017), thus the activity of 2a and 2b can be categorized as moderate. However, they are inactive against *B. subtilis.* Therefore, only four bacterial strains were selected for further testing using the microdilution method to obtain a more precise quantitative measure of antibacterial potency.

The result for *in vitro* evaluation using the microdilution (Table IIB). The higher antibacterial activity of a compound was indicated by the low MIC50 value.

Table II. *In vitro* antibacterial activity evaluation

A. Disk Diffusion Method					
Compounds (1000 µg/mL)	**Inhibition zones (mm)**				
	S. aureus	***S. epidermidis***	***B. subtilis***	***E. coli***	***P. aeruginosa***
2a	9	7	-	7	7
2b	9	-	-	7	7
Ciprofloxacin	30	31	31	41	33
DMSO 1%	-	-	-	-	-
B. Microdilution Method					
Compounds	**MIC50* (µg/mL)**				
	S. aureus	***S. epidermidis***	***B. subtilis***	***E. coli***	***P. aeruginosa***
2a	$95.78 \pm 3.94^{a,1}$	>1000	n.d.	$613.62 \pm 18.38^{b,1}$	>1000
2b	$71.64 \pm 2.31^{a,2}$	>1000	n.d.	$676.77 \pm 27.45^{b,2}$	$568.99 \pm 9.51^{c,1}$
Ciprofloxacin	$0.014 \pm 0.001^{a,3}$	0.243 ± 0.005^{a}	n.d.	$0.083 \pm 0.005^{a,3}$	$0.008 \pm 0.001^{b,2}$

*Different superscript letters within the same row represent statistically significant differences ($p < 0.01$) based on one-way ANOVA with Tukey's post hoc test applied. Different superscript numbers within the same column represent statistically significant differences ($p < 0.05$). "n.d." = not determined.

The evaluation against two Gram-positive bacteria showed that both compounds 2a-b have significantly ($p < 0.01$) higher growth inhibition activity against *S. aureus* compared to their activity against *S. epidermidis*, as indicated by their lower MIC_{50} values. This may be caused by the thickness differences in the peptidoglycan layer within the bacterial cell wall. Both *S. aureus* and *S. epidermidis* are Gram-positive bacteria with a thick peptidoglycan layer, however the thickness of peptidoglycan in *S. epidermidis* was reported to be twice that of *S. aureus* (Sharif et al., 2009; Sanyal & Greenwood, 1993). Thus, it might reduce the penetration of compounds 2a-b and lead to lower susceptibility of *S. epidermidis.* Compound 2b, bearing a phenyl group on the N-1 position of the pyrazoline ring, demonstrated stronger activity against *S. aureus* compared to 2a with a more polar formyl group. While Gram-positive bacteria typically allow easier penetration of hydrophilic molecules (Tavares et al., 2020), the higher activity of 2b may be due to the aromatic phenyl ring that can enhance interactions with hydrophobic regions of intracellular targets, such as DNA gyrase (Bakker et al., 2024). The evaluation against two Gram-negative bacteria *E. coli* and *P. aeruginosa* showed that both compounds 2a and 2b have significantly ($p < 0.01$) lower growth inhibition activity compared to that against Gram-positive *S. aureus.* This reduced activity is consistent with the differences in the structure of the cell envelope, where Gram-negative bacteria possess an outer membrane that serves as a barrier to many antibiotics (Maher & Hassan, 2023).

The categorization of antibacterial potency based on MIC_{50} values is not universally standardized, however several studies have proposed threshold ranges based on MIC values to categorize the activity levels. For instance, MIC values <100 µg/mL are generally considered as strong, 100-625 µg/mL as moderate, 625-1000 µg/mL as weak, and >1000 µg/mL as inactive (Wamba et al., 2018; dos Santos et al., 2023). Therefore, MIC_{50} values on compounds 2a and 2b against *S. aureus* (<100 µg/mL) may be interpreted as strong activity, while MIC_{50} values in the range of 100-1000 µg/mL, such as those of compound 2a and 2b against *E. coli* and compound 2b against *P. aeruginosa*, suggest moderate activity.

These results showed that both styrylpyrazolines 2a and 2b exhibited antibacterial activity against certain bacterial strains. The most notable activity was observed against *S. aureus.* Although their potency is significantly lower compared to the standard antibiotic ciprofloxacin, the results support their potential as lead compounds for further structural modification toward antibacterial agents, particularly those targeting Gram-positive *S. aureus.*

Molecular Docking Study

Since the strongest antibacterial activity was found against *S. aureus*, molecular docking of styrylpyrazolines 2a-2b was performed on its DNA gyrase subunit B (GyrB) to predict their interaction. The protein used in this study was the ATP domain of GyrB. ATP is essential for the activation of GyrB.

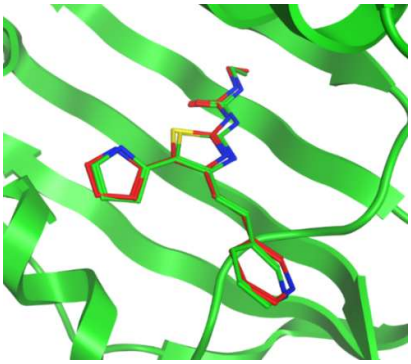

Figure 2. Alignment between co-crystallized 57V (green) and 57V from redocking result (red)

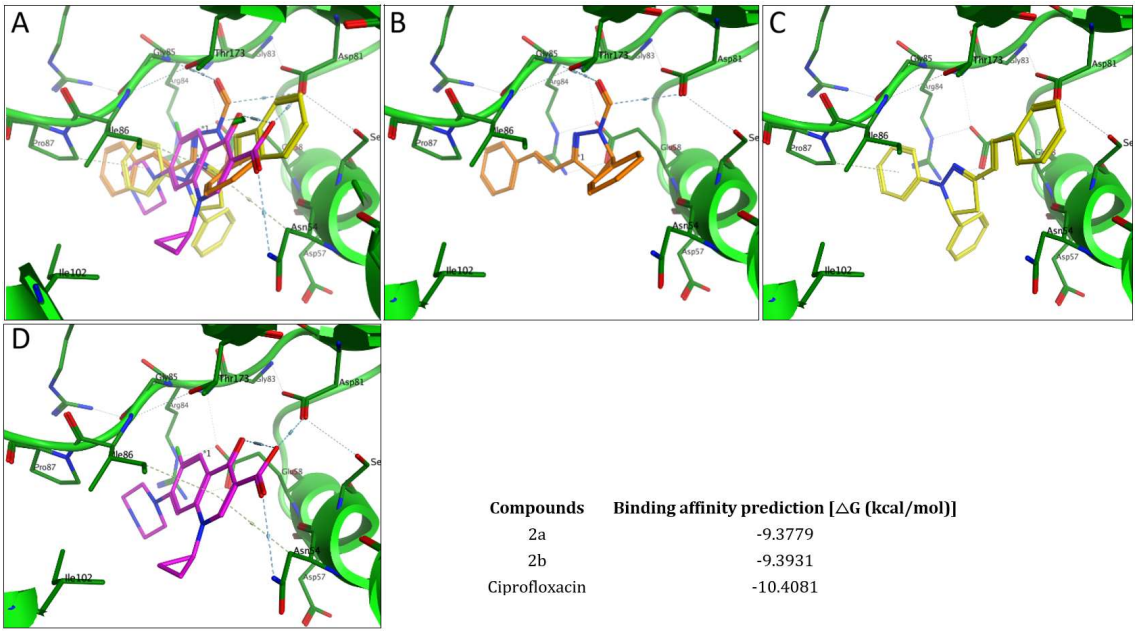

Compounds	Binding affinity prediction [△G (kcal/mol)]
2a	-9.3779
2b	-9.3931
Ciprofloxacin	-10.4081

Figure 3. Three-dimensional visualization of the compounds–amino acid residues interaction in the binding site and the molecular docking results. (A) Superimposed binding interaction of compound 2a (orange), compound 2b (yellow), and ciprofloxacin (magenta), (B) binding interaction of compound 2a, (C) binding interaction of compound 2b, and (D) binding interaction of ciprofloxacin

It induces conformational changes necessary for converting the clamp-like structure from an open form to a closed state capable of holding a DNA molecule and transferring it to the holoprotein structure (Gupta, 2021). The reliability of the docking protocol was confirmed through a redocking validation step, in which the co-crystallized ligand (compound 57V) was redocked into the active site of the receptor. The resulting root-mean-square deviation (RMSD) value of redocking was 0.3110 Å. This value was less than 2 Å, so it was considered as accurately reproduced ligand positioning and indicated that the docking protocol was valid for performing further molecular docking analysis (Khachatryan et al., 2024). The binding affinity prediction (△G) for the redocked ligand was -9.6997 kcal/mol, further supporting the reliability of the docking setup. The 3D visualization (Figure 2) also confirmed that the co-crystallized 57V and 57V from redocking results were well aligned.

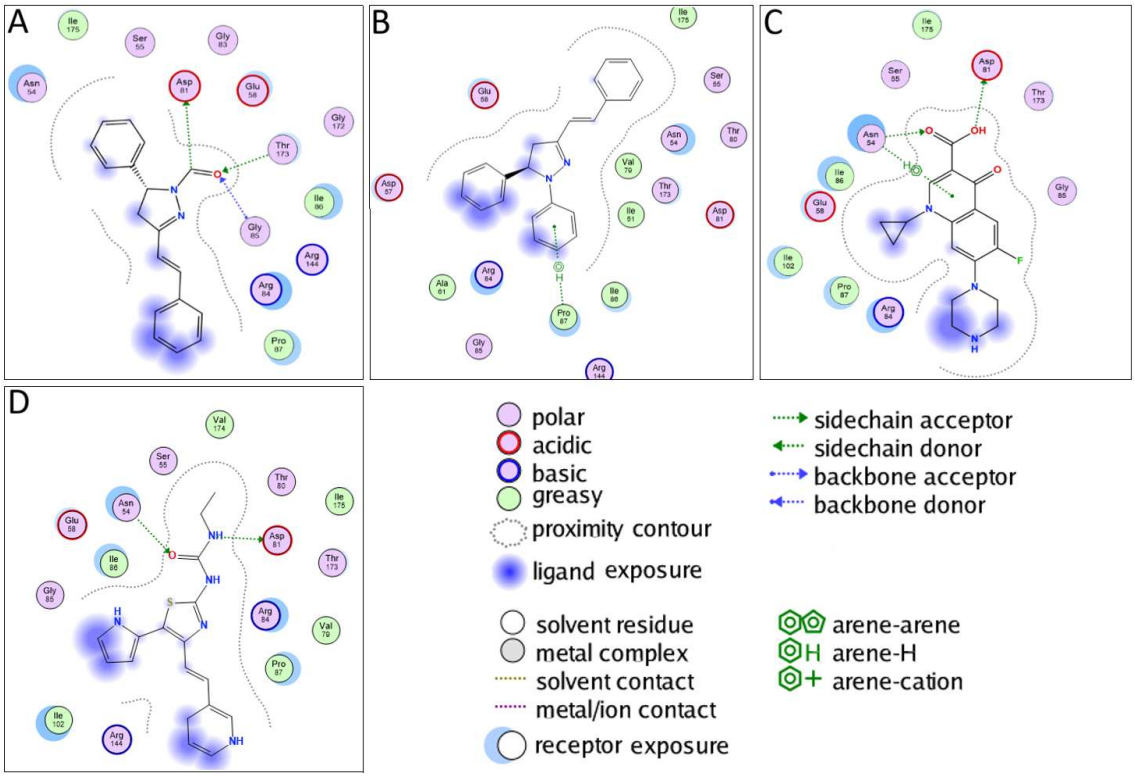

Compounds	Amino acid residues in the binding site	Interaction type
2a	Ile51, Asn54, Ser55, Glu58, Val79, Thr80, Asp81, Arg84, Gly85, Pro87, Ile88, Ile102, Arg144, Val174, Ile175, Thr173	H bond with Asp81, Thr173, Gly85 Aromatic-H bond with Pro87
2b		
Ciprofloxacin		H Bond with Asn54, Asp81, aromatic-H bond with Asn54
57V		

Figure 4. Two-dimensional visualization and a list of interactions between compounds with the amino acid residues in the binding site. (A) compound 2a, (B) compound 2b, (C) ciprofloxacin, and (D) 57V

From the molecular docking analysis, binding affinity prediction can be estimated through docking results (Pantsar & Poso, 2018). The molecular docking result presented in Figure 3 indicated that compounds 2a and 2b exhibit sufficient stability in binding to the target site, with binding affinity values of -9.3779 and -9.3931 kcal/mol, respectively. Compared to ciprofloxacin, the docking scores for compounds 2a and 2b were lower. Ciprofloxacin demonstrated strong inhibition across all tested bacteria, suggesting that the docking results correspond to the *in vitro* findings. Despite having lower activities, compounds 2a and 2b may still exhibit antibacterial properties by inhibiting GyrB. Figure 3 also depicts the docking poses of ciprofloxacin, compound 2a, and compound 2b. All compounds occupied the hinge region at the ATP binding site, located deep within the pocket. GyrB, a subtype of gyrase, possesses ATPase activity, providing the energy required for DNA cleavage.

Consequently, compounds 2a and 2b may block the ATP binding to GyrB, like ciprofloxacin, thereby inhibiting DNA replication. Figure 4 shows the 2D visualization and lists the amino acid residues involved in ATP binding, as well as the interactions of compounds with these residues. Similar to native ligand and ciprofloxacin, compound 2a interacts with the Asp81 residue through hydrogen bonding and two additional interactions with Thr173 and Gly85 residues due to the presence of a formyl group in the N-1 position of the pyrazoline ring. Compound 2b, which bears three aromatic rings, formed aromatic-hydrogen bridging with the Pro87 residue on the phenyl group in the N-1 position of the pyrazoline rings.

This aromatic-hydrogen bridging was also present in ciprofloxacin. These results confirmed that both compounds 2a and 2b were able to interact with some of the key residues in the ATP-binding pocket, and the presence of a functional group in the N-1 position of the pyrazoline ring serves as a crucial factor in influencing their binding interactions and stability within the active site.

Although the styrylpyrazoline derivatives investigated in this study showed antibacterial activity and were able to interact with DNA gyrase subunit B, their lower potency relative to ciprofloxacin and their weaker activity against Gram-negative bacteria indicate that further optimization is still needed. In this regard, structural modification remains an important strategy for improving the antibacterial potency of these compounds. In addition, drug delivery systems may also be considered in future studies as a complementary approach to support the therapeutic performance of promising styrylpyrazoline-based antibacterial agents (Pelgrift & Friedman, 2013).

CONCLUSION

The findings of this study indicate that N-1 substitution plays an important role in determining the antibacterial activity of styrylpyrazoline derivatives. The stronger activity of compound 2b against *S. aureus*, together with the observed interactions of both compounds with key residues in the ATP-binding pocket of DNA gyrase subunit B, supports the relevance of the styrylpyrazoline scaffold as a potential antibacterial lead. Nevertheless, the lower potency relative to ciprofloxacin suggests that further optimization is still required to improve its antibacterial performance.

ACKNOWLEDGMENTS

This study was financially supported by the Faculty of Pharmacy, Universitas Gadjah Mada, via the research project of Penelitian Kolaborasi Nasional 2024 (Grant No. 6.22/UN1/FA.1/SETPIM/PT/2024).

CONFLICT OF INTEREST

The authors state that there is no conflict of interest.

REFERENCES

Adeniji, S. E., Adalumo, O. B., & Ekoja, F. O. (2020). Anti-tubercular modelling, molecular docking simulation and insight toward computational design of novel compounds as potent antagonist against DNA gyrase receptor. *Medicine in Microecology*, 5, Article 100020. https://doi.org/10.1016/j.medmic.2020.100020

Alex, J. M., & Kumar, R. (2014). 4,5-Dihydro-1H-pyrazole: An indispensable scaffold. *Journal of Enzyme Inhibition and Medicinal Chemistry*, 29(3), 427–442. https://doi.org/10.3109/14756366.2013.795956

Bakker, A. T., Kotsogianni, L., Avalos, M., Punt, J. M., Liu, B., Piermarini, D., Gagestein, B., Slingerland, C. J., Zhang, L., Willemse, J. J., Ghimire, L. B., van den Berg, R. J. H. B. N., Janssen, A. P. A., Ottenhoff, T. H. M., van Boeckel, C. A. A., van Wezel, G. P., Ghilarov, D., Martin, N. I., & van der Stelt, M., (2024). Discovery of isoquinoline sulfonamides as allosteric gyrase inhibitors with activity against fluoroquinolone-resistant bacteria. *Nature Chemistry*, 16(9), 1462-1472. https://doi.org/10.1038/s41557-024-01516-x

Balouiri, M., Sadiki, M., & Ibnsouda, S. K. (2016). Methods for in vitro evaluating antimicrobial activity: A review. *Journal of Pharmaceutical Analysis*, 6(2), 71-79. https://doi.org/10.1016/j.jpha.2015.11.005

Casalini, T. (2021). Not only in silico drug discovery: Molecular modeling towards in silico drug delivery formulations. *Journal of Controlled Release*, 332, 390-417. https://doi.org/10.1016/j.jconrel.2021.03.005

Clinical and Laboratory Standards Institute (CLSI). (2023). *Performance standards for antimicrobial susceptibility testing* (33rd ed.). CLSI supplement M100. https://clsi.org/media/tc4b1paf/m10033_samplepages-1.pdf

Cvijic, S., Ibric, S., Parojcic, J., & Djuris, J. (2018). An in vitro - in silico approach for the formulation and characterization of ranitidine gastroretentive delivery systems. *Journal of Drug Delivery Science and Technology*, 45, 1-10. https://doi.org/10.1016/j.jddst.2018.02.013

Dos Santos, É. L., Santana, A. C., Micheletti, A. C., Freire, T. V., Guterres, Z. R., & Yoshida, N. C. (2023). Metabolomic profiling and

assessment of antimicrobial, antioxidant and genotoxic potential of Unonopsis guatterioides R.E.Fr. (Annonaceae) fruits. *Arabian Journal of Chemistry*, 16, Article 105133. https://doi.org/10.1016/j.arabjc.2023.105133

Gomes, P. M. O., Ouro, P. M. S., Silva, A. M. S., & Silva, V. L. M. (2020). Styrylpyrazoles: Properties, synthesis and transformations. *Molecules*, 25(24), Article 5886. https://doi.org/10.3390/molecules25245886

Gressler, V., Moura, S., Flores, A. F. C., Flores, D. C., Colepicolo, P., & Pinto, E. (2010). Antioxidant and antimicrobial properties of 2-(4,5-dihydro-1H-pyrazol-1-yl)-pyrimidine and 1-carboxamidino-1H-pyrazole derivatives. *Journal of the Brazilian Chemical Society*, 21(8), 1477–1483. https://doi.org/10.1590/S0103-50532010000800010

Gupta, D., Tiwari, P., Haque, M. A., Sachdeva, E., Hassan, M. I., Ethayathulla, A. S., & Kaur, P. (2021). Structural insights into the transient closed conformation and pH dependent ATPase activity of S.Typhi GyraseB N-terminal domain. *Archives of biochemistry and biophysics*, 701, Article 108786. https://doi.org/10.1016/j.abb.2021.108786

Ho, C. S., Wong, C. T. H., Aung, T. T., Lakshminarayanan, R., Mehta, J. S., Rauz, S., McNally, A., Kintses, B., Peacock, S. J., de la Fuente-Nunez, C., Hancock, R. E. W., & Ting, D. S. J. (2025). Antimicrobial resistance: A concise update. *The Lancet Microbe*, 6(1), Article 100947. https://doi.org/10.1016/j.lanmic.2024.07.010

Hooper, D. C. & Jacoby, G. A. (2016). Topoisomerase inhibitors: Fluoroquinolone mechanisms of action and resistance. *Cold Spring Harbor Perspective in Medicine,* 6(9), Article a025320. https://doi.org/10.1101/cshperspect.a025320

Houshia, O., Walwil, A., Jumaa, H., Qrareya, H., Daraghmeh, H., Daraghmeh, I., Owies, A., & Qushtom, A. (2019). Assessment of the ratio of geometric isomers of dibenzalacetone spectroscopically. *Journal of Pharmaceutical Research International*, 31(4), 1–9. https://doi.org/10.9734/JPRI/2019/v31i430307

Khachatryan, H., Matevosyan, M., Harutyunyan, V., Gevorgyan, S., Shavina, A., Tirosyan, I., Gabrielyan, Y., Ayvazyan, M., Bozdaganyan, M., Fakhar, Z., Gharaghani, S., & Zakaryan, H. (2024). Computational evaluation and benchmark study of 342 crystallographic holo-structures of SARS-CoV-2 Mpro enzyme. *Scientific Reports,* 14(1), Article 14255. https://doi.org/10.1038/s41598-024-65228-5

Maher, C. & Hassan, K. A. (2023). The Gram-negative permeability barrier: Tipping the balance of the in and the out. *mBio*, 14(6), Article e01205-23. https://doi.org/10.1128/mbio.01205-23

Marshall, C. M., Federice, J. G., Bell, C. N., Cox, P. B., & Njardarson, J. T. (2024). An update on the nitrogen heterocycle compositions and properties of U.S. FDA-approved pharmaceuticals (2013-2023). *Journal of Medicinal Chemistry*, 67(14), 11622-11655. https://doi.org/10.1021/acs.jmedchem.4c01122

Molecular Operating Environment (MOE), (2022). 2022.02; Chemical Computing Group ULC, 1010 Sherbrooke St. West, Suite #910, Montreal, QC, Canada, H3A 2R7.

Nassan, M. A., Aldhahrani, A., Amer, H. H., Elhenawy, A., Swelum, A. A., Ali, O. M., & Zaki, Y. H. (2022). Investigation of the anticancer effect of α-aminophosphonates and arylidine derivatives of 3-acetyl-1-aminoquinolin-2(1H)-one on the DMBA model of breast cancer in albino rats with in silico prediction of their thymidylate synthase inhibitory effect. *Molecules*, 27(3), Article 756. https://doi.org/10.3390/molecules27030756

Pantsar, T., & Poso, A. (2018). Binding affinity via docking: Fact and fiction. *Molecules*, 23(8), Article 1899. https://doi.org/10.3390/molecules23081899

Pelgrift, R. Y., & Friedman, A. J. (2013). Nanotechnology as a therapeutic tool to combat microbial resistance. *Advanced Drug Delivery Reviews*, 65(13-14), 1803-1815. https://doi.org/10.1016/j.addr.2013.07.011

Sanyal, D., & Greenwood, D. (1993). An electronmicroscope study of glycopeptide antibiotic-resistant strains of

Staphylococcus epidermidis. *Journal of Medical Microbiology*, 39(3), 204–210. https://doi.org/10.1099/00222615-39-3-204

Sharif, S., Singh, M., Kim, S. J., & Schaefer, J. (2009). Staphylococcus aureus peptidoglycan tertiary structure from carbon-13 spin diffusion. *Journal of the American Chemical Society,* 131(20), 7023–7030. https://doi.org/10.1021/ja808971c

Sharma, B. K., Dwivedi, V. K., Ameta, S. C., & Rao, D. (2013). Microwave induced synthesis and antimicrobial activities of some substituted chalcones and their pyrazoline and isoxazoline derivatives. *International Journal of Chemical Sciences*, 11(2), 1086–1094.

Shi, Z., Zhang, J., Tian, L., Xin, L., Liang, C., Ren, X., & Li, M. (2023). A comprehensive overview of the antibiotics approved in the last two decades: Retrospects and prospects. *Molecules*, 28(4), Article 1762. https://doi.org/10.3390/molecules28041762

Sid, A., Messai, A., Parlak, C., Kazancı, N., Luneau, D., Keşan, G., Rhyman, L., Alswaidan, I. A., & Ramasami, P. (2016). 1-Formyl-3-phenyl-5-(4-isopropylphenyl)-2-pyrazoline: Synthesis, characterization, antimicrobial activity, and DFT studies. *Journal of Molecular Structure,* 1121, 46–53. https://doi.org/10.1016/j.molstruc.2016.05.043

Singh, P., Negi, J. S., Pant, G. J. N., Rawat, M. S. M., & Budakoti, A. (2009). Synthesis and characterization of a novel 2-pyrazoline. *Molbank*, 2009(3), Article M614. https://doi.org/10.3390/M614

Suma, A. A. T., & Wahyuningsih, T. D. (2023). Study of 1-formyl-2-pyrazolines as anticancer drug candidates. *Indonesian Journal of Pharmacy*, 34(4), 630–639. https://doi.org/10.22146/ijp.7188

Suma, A. A. T., Wahyuningsih, T. D., & Mustofa. (2019). Synthesis, cytotoxicity evaluation, and molecular docking study of N-phenylpyrazoline derivatives. *Indonesian Journal of Chemistry*, 19(4), 1081–1090. https://doi.org/10.22146/ijc.45777

Suma, A. A. T., Wahyuningsih, T. D., & Pranowo, D. (2017). Synthesis and antibacterial activities of N-phenylpyrazolines from veratraldehyde. *Materials Science Forum,* 901, 124–132. https://doi.org/10.4028/www.scientific.net/MSF.901.124

Torres, P. H. M., Sodero, A. C. R., Jofily, P., & Silva-Jr, F. P. (2019). Key topics in molecular docking for drug design. *International Journal of Molecular Sciences*, 20(18), Article 4574. https://doi.org/10.3390/ijms20184574

Uddin, T. M., Chakraborty, A. J., Khusro, A., Zidan, B. M. R. M., Mitra, S., Emran, T. B., Dhama, K., Ripon, M. K. H., Gajdács, M., Sahibzada, M. U. K., Hossain, M. J., & Koirala, N. (2021). Antibiotic resistance in microbes: History, mechanisms, therapeutic strategies and future prospects. *Journal of Infection and Public Health,* 14(12), 1750–1766. https://doi.org/10.1016/j.jiph.2021.10.020

Vahedpour, T., Hamzeh-Mivehroud, M., Hemmati, S., & Dastmalchi, S. (2021). Synthesis of 2-pyrazolines from hydrazines: Mechanisms explained. *ChemistrySelect*, 6(25), 6483–6506. https://doi.org/10.1002/slct.202101467

Varghese, B., Al-Busafi, S. N., Suliman, F. O., & Al-Kindy, S. M. Z. (2017). Unveiling a versatile heterocycle: pyrazoline – a review. *RSC Advances*, 7, 46999-47016. https://doi.org/10.1039/C7RA08939B

Wamba, B. E. N., Nayim, P., Mbaveng, A. T., Voukeng, I. K., Dzotam, J. K., Ngalani, O. J. T., & Kuete, V. (2018). Syzygium jambos displayed antibacterial and antibiotic-modulating activities against resistant phenotypes. *Evidance-Based Complementary and Alternative Medicine,* 2018(1), Article 5124735. https://doi.org/10.1155/2018/5124735

World Health Organization, Food and Agriculture Organization of the United Nations, & World Organisation for Animal Health. (2019). *Monitoring and evaluation of the global action plan on antimicrobial resistance: Framework and recommended indicators*. World Health Organization. https://iris.who.int/handle/10665/325006

Yadav, C. S., Azad, I., Khan, A. R., Nasibullah, M., Ahmad, N., Hansda, D., Ali, S. N., Shrivastav, K., Akil, M., & Lohani, M. B. (2024). Recent advances in the synthesis of pyrazoline derivatives from chalcones as potent pharmacological agents: A comprehensive review. *Results in Chemistry*, 7, Article 101326. https://doi.org/10.1016/j.rechem.2024.101326

Zhang, J., Yang, Q., Cross, J. B., Romero, J. A. C., Poutsiaka, K. M., Epie, F., Bevan, D., Wang, B., Zhang, Y., Chavan, A., Zhang, X., Moy, T., Daniel, A., Nguyen, K., Chamberlain, B., Carter, N., Shotwell, J., Silverman, J., Metcalf, C. A., … Dolle, R. E. (2015). Discovery of azaindole ureas as a novel class of bacterial gyrase B inhibitors. *Journal of Medicinal Chemistry,* 58(21), 8503–8512. https://doi.org/10.1021/acs.jmedchem.5b00961